

NASA Technical Memorandum 107209

# Prediction of In-Space Durability of Protected Polymers Based on Ground Laboratory Thermal Energy Atomic Oxygen

Bruce A. Banks, Kim K. de Groh, Sharon K. Rutledge  
*Lewis Research Center*  
*Cleveland, Ohio*

Frank J. DiFilippo  
*Case Western Reserve University*  
*Cleveland, Ohio*

Prepared for the  
Third International Conference for Protection of Materials and Structures  
from the LEO Space Environment  
sponsored by the Canadian Space Agency and the Institute for  
Space and Terrestrial Studies  
Toronto, Canada, April 25–26, 1996



National Aeronautics and  
Space Administration

Trade names or manufacturers' names are used in this report for identification only. This usage does not constitute an official endorsement, either expressed or implied, by the National Aeronautics and Space Administration.

# **PREDICTION OF IN-SPACE DURABILITY OF PROTECTED POLYMERS BASED ON GROUND LABORATORY THERMAL ENERGY ATOMIC OXYGEN**

**Bruce A. Banks, Kim K. de Groh, and Sharon K. Rutledge**

**NASA Lewis Research Center  
Cleveland, Ohio  
and**

**Frank J. DiFilippo**

**Case Western Reserve University  
Cleveland, Ohio**

## **ABSTRACT**

The probability of atomic oxygen reacting with polymeric materials is orders of magnitude lower at thermal energies ( $<0.1$  eV) than at orbital impact energies (4.5 eV). As a result, absolute atomic oxygen fluxes at thermal energies must be orders of magnitude higher than orbital energy fluxes, to produce the same effective fluxes (or same oxidation rates) for polymers. These differences can cause highly pessimistic durability predictions for protected polymers and polymers which develop protective metal oxide surfaces as a result of oxidation if one does not make suitable calibrations. A comparison was conducted of undercut cavities below defect sites in protected polyimide Kapton samples flown on the Long Duration Exposure Facility (LDEF) with similar samples exposed in thermal energy oxygen plasma. The results of this comparison were used to quantify predicted material loss in space based on material loss in ground laboratory thermal energy plasma testing. A microindent hardness comparison of surface oxidation of a silicone flown on the Environmental Oxygen Interaction with Materials-III (EOIM-III) experiment with samples exposed in thermal energy plasmas was similarly used to calibrate the rate of oxidation of silicone in space relative to samples in thermal energy plasmas exposed to polyimide Kapton effective fluences.

## **INTRODUCTION**

The atomic oxygen durability of polymers in low Earth orbit (LEO) that are protected by means of thin films is predominantly dependent upon the rate of mass loss associated with atomic oxygen undercutting at defect sites in the protective coatings (Ref. 1). Typical defects include pin windows and scratches or cracks in the protective coatings caused by initial surface

irregularities of the unprotected material, contamination during the deposition process, dust or debris on the surfaces occurring prior to deposition, processing and handling damage, and in-space damage associated with micrometeoroid and debris impacts (Ref. 2). Atomic oxygen impinging on protected polymers at defect sites in the protective coating is able to react with the exposed polymer thus producing gaseous reaction products for typical hydrocarbon polymers such as polyimide Kapton used for solar array blankets. The atomic oxygen erosion, however, is not simply limited to polymer surfaces that are within the line of sight of the arriving atomic oxygen. This is because of scattering of unreacted atomic oxygen which enables additional opportunities for oxygen reaction at locations which may be out of the line of sight of the original arriving atoms. The degree of atomic oxygen undercutting would, of course, depend upon the directional characteristics of the arriving atomic oxygen in addition to other scattering characteristics. Fixed direction atomic oxygen arrival should produce narrower undercutting than sweeping or isotropic arrival of atomic oxygen (Ref. 3).

The durability of a protected polymer in space is frequently dependent upon its potential for structural failure such as the breaking or tearing under tension as would occur for a solar array blanket. This catastrophic failure is usually a greater risk than unacceptable changes in thermal properties such as emittance or absorptance. Thus, the in-space durability of protected polymers depends not only upon the expected flux but the nature of the arrival direction of atomic oxygen (fixed or sweeping arrival).

The in-space durability of polymers that develop protective oxides such as silicones and polyarylene ether benzimidazole (PAEBI) is similarly dominated by structural integrity issues associated with breaking or tearing of these materials while under stress. However, the failure mode of materials which develop protective oxides is different, in that there is a gradual conversion of the material to a metal oxide. This begins on the exposed surface with the oxide growing in depth with atomic oxygen fluence (Ref. 4-6). For such materials the undercutting of defect sites is not an issue, but instead gradual embrittlement and/or potential crazing becomes the dominant mode of failure. For such degradation processes it is probable that the differences in the consequences associated with sweeping versus direct ram atomic oxygen arrival may be much less apparent or indistinguishable.

For most protected polymers and polymers which develop protective oxides, the rate of erosion or degradation is dependent upon the atomic oxygen flux and the probability of reaction of impinging atomic oxygen. The probability of atomic oxygen reaction depends upon mechanistic considerations including oxygen atom energy, angle of attack, and other oxygen atom/material interaction properties. These properties regulate oxidation consequences in undercut cavities below defect sites for protected polymers and in the microscopic pores of polymers that develop protective oxides. Some of the detailed oxygen polymer interaction processes which may control rates of oxidation include probability of atomic oxygen recombination, degree of thermal accommodation of rejected and unreacted atomic oxygen and the angular distribution of unreacted scattered atomic oxygen. To be able to predict in-space durability based on ground laboratory testing, one must accelerate the rates of degradation to obtain practical information in a reasonable duration. However, one must also understand the consequences of the

differences between the ground laboratory exposure conditions and those which occur in space to be able to quantifiably predict in-space durability. The qualification of materials needed for high atomic oxygen fluence missions such as the International Space Station and the Tropical Rainfall Measuring Mission have required sample sizes for post-exposure engineering evaluation which would have been prohibitively expensive to expose in energetic beam facilities. As a result, the preponderance of such testing has occurred through broad area thermal energy directed beam plasma exposure. Thus, the challenge to predict in-space durability based on such tests is highly dependent upon the consequences of the differences in oxygen impact energies.

In low Earth orbit, under the ideal circumstance of a fixed ram atomic oxygen exposure, the impact energy of arriving atomic oxygen is distributed. This distribution is a result of Maxwellian distribution of speeds of the hot thermospheric atoms and the addition of adding velocity vectors associated with the spacecraft orbital velocity having an inclination relative to the Earth's atmospheric co-rotation velocity. As a result, a LEO atomic oxygen impact energy distribution is produced with a mean energy of 4.5 eV +/- 1 eV for 28.5° inclined orbits at 400 km altitudes, assuming an atmospheric temperature of 996 K (see Figure 1) (Ref. 7). The mean energy varies only slightly with altitude as is shown in Figure 2 (Ref. 7). The same characteristics of the arriving atomic oxygen which cause a variation in the arrival energy, also contribute to an angular distribution of arrival flux. As can be seen in Figure 3 (data in Table I), the angular distribution of arriving atomic oxygen flux for both a plane parallel to the Earth's horizon as well as a plane perpendicular to the Earth's horizon are quite similar with the preponderance of the flux arriving within a cone half angle of 18°.

In contrast to the high energy arrival in space, thermal energy ground laboratory simulation systems have impact energies typically below 0.1 eV. Investigators have found that the probability of atomic oxygen reaction is highly dependent upon the impact energy (Ref. 8 and 9). The results of four investigators report atomic oxygen erosion yield dependencies proportional to the impact energy raised to a power ranging from 0.68 to 2.7 for polyimide Kapton. Thus, simulation of LEO atomic oxygen erosion at accelerated rates using thermal energy atoms requires enormously enhanced atomic oxygen fluxes compared to that in LEO because of the orders of magnitude lower erosion yields.

Typical ground laboratory atomic oxygen testing is calibrated by means of polyimide Kapton witness coupons which are exposed along with the test samples to measure the effective atomic oxygen fluence. The effective atomic oxygen fluence measured in the ground laboratory exposure facility is equal to the atomic oxygen fluence in LEO which would cause the same amount of oxidation (thickness loss for Kapton polyimide) as observed in the ground laboratory environment (Ref. 10). Thus, effective fluence is the in-space fluence which causes equivalent damage for unprotected materials, either in the space or laboratory environment independent of atomic oxygen energy. Although this calibration works well for uncoated materials provided the erosion yield (volume loss per incident atom) is known in LEO for each material, the consequences of the atomic oxygen energy differences complicate lifetime predictions for protected polymers or polymers which develop protective oxides. As illustrated in Figure 4, simulation of the LEO environment by means of an isotropic thermal energy plasma requires a

significantly higher atomic oxygen flux than LEO because the reaction probability for thermal energy atoms is so low. Although both the in-space and laboratory environment unprotected polymers have the same amount of erosion (same equivalent fluence), the degree of atomic oxygen undercutting at defect sites in the protective coating differs greatly between defect sites in space and defect sites in a thermal energy oxygen plasma. This is because atoms which enter a defect cavity at high energies in the LEO environment are thought to have an initial impact reaction probability of approximately 14%, but upon scattering and thermal accommodation rapidly lose reaction probability to become relatively ineffective at oxidation. Thus, the in-space atomic oxygen tends to drill in deep with much less undercutting (due to secondary reaction events) than the ground laboratory atomic oxygen interactions at defect sites. In the ground laboratory environment, high abundances of thermal energy atomic oxygen is needed to simulate the same effective fluences as in space; however, because the atoms are already nearly thermally accommodated, their great abundance causes secondary impact of atomic oxygen erosion in undercut cavities to create much wider undercut cavities than would occur for the same defects in LEO. These same issues occur on a much more molecular level for polymers that develop protective oxides such as silicones and PAEBI's.

The objective of this investigation is to compare the degree of undercutting for similar size protective coating defects exposed to LEO and ground laboratory thermal energy plasma environments in order to predict in-space durability based on ground laboratory thermal energy plasma testing. Because polymers which develop protective oxides cannot be calibrated in this manner, a comparison of surface hardness was used for calibrating ground laboratory thermal energy plasma exposures to enable quantified prediction of in-space durability of these materials.

## **Apparatus and Procedure**

### Protected Polymers Which Produce Volatile Oxides

Although the below described apparatus and procedure involved the use of polyimide Kapton H which was protected by a thin aluminum film, the techniques used are applicable to any material whose oxides are fully volatile and the material is protected by means of a thin oxidation resistant film. Ideally, to make a correlation between in-space and ground laboratory thermal energy plasma durability, one would like to compare the mass loss of a protected polymer exposed to high atomic oxygen fluence in space with mass loss of the identical material exposed to the same effective fluence in a ground laboratory thermal energy exposure system. However, because protected polymers exposed in space could have very low oxidation rates, the uncertainties in the predicted in-space durability exist because of the shortage of reliable high-fluence data. For example, data from samples retrieved from the STS-8 mission, having an estimated fluence of  $3.5 \times 10^{20}$  atoms/cm<sup>2</sup> indicated that Kapton H protected with SiO<sub>2</sub>,  $\geq 96\%$  SiO<sub>x</sub>,  $\leq 4\%$  PTFE, and Al<sub>2</sub>O<sub>3</sub> had relative reactivities with respect to unprotected Kapton H of 0.0012, 0.002, and 0.113 respectively (Ref. 11). Such low rates of oxidation of protected Kapton indicates that in-space testing on missions having an atomic oxygen fluence of  $> 7.5 \times 10^{20}$  atoms/cm<sup>2</sup> is required to be able to have in-space mass losses measured which exceed the measured probable error in mass loss of  $1.24 \times 10^{-5}$  grams for typical 2.54 cm diameter,

0.00254 cm thick protected polymer samples with an exposed diameter of 2.06 cm. Because this fluence exceeds typical shuttle missions, the only high fluence data obtainable was taken from protected samples exposed to high fluence on LDEF. The LDEF sample consisted of a 0.00254 cm thick Kapton H substrate which was coated with approximately 1000 Å of aluminum on the space exposed surface (Ref. 12). The sample was part of the LDEF experiment AO171, and was loaded on row 8-A and thus was flown such that atomic oxygen arrived at 38.1° from the normal incidence direction (Ref. 13). With the LDEF ram fluence being  $9.09 \times 10^{21}$  atoms/cm<sup>2</sup>, the off-normal component of the fluence on the sample was  $7.15 \times 10^{21}$  atoms/cm<sup>2</sup> (Ref. 14). Although this fluence is more than adequate to obtain meaningful mass loss data based on previous low fluence data (Ref. 11), no pre-flight mass measurement had been made, thus inhibiting this approach to determining the in-space mass loss. Rather than comparing in-space versus plasma mass loss, an approach was used which was intended to produce these same results by measurement of the volume of the undercut cavities associated with nearly identical area defects for both the LDEF exposure and ground laboratory plasma asher exposure, the premise being that for a typical pin window defect, the ratio of the in-space undercut volume to the plasma asher undercut volume should be proportional to the overall mass loss rates. This approach was accomplished by preparation of a similar 0.00254 cm thick aluminized Kapton H sample which was exposed in a ground laboratory plasma asher to the same atomic oxygen effective fluence ( $7.15 \times 10^{21}$  atoms/cm<sup>2</sup>) as the LDEF sample. The two samples were then inspected by scanning electron microscopy to identify nearly identical area pin window defects in each sample. The pin window defects were photographed and then the aluminized film was chemically removed using dilute hydrochloric acid to expose the respective undercut cavities. Further, scanning electron microscopy at various viewing angles was then performed to quantify the shape, depth and diameter of the undercut cavities of each sample.

#### Polymers that develop protective oxides

The in-space durability of quasi-durable materials such as silicones and PAEBI's cannot be determined by the same procedure as used for polymers and materials which produce volatile oxides, because these materials have a mix of both volatile oxides and non-volatile oxides as a result of atomic oxygen attack. The combined processes of producing both volatile as well as non-volatile oxides cause the mass loss of these materials to be a very poor indicator of durability. For example, some materials show almost negligible mass change yet there may be a near complete conversion of the material to an oxide such as silica in the case of a silicone polymer or phosphorous in the case of PAEBI's which results in the material being unsuitable for bonding components or as a structural blanket (Ref. 5). Thus, even though the mass loss may be negligible, the material's structural durability would be unacceptable. In the case of silicones, the modulus of elasticity of the surface of the silicone gradually increases as the silicone is oxidized to become a predominantly silica surface. As the silicone becomes oxidized to a deeper depth the stiffness of the surface increases and can be qualified by using atomic force microscopy to measure the force necessary to push a stylus into the surface for a fixed penetration distance. As one would expect, the indent force per indent distance increases with atomic oxygen fluence. Calibration of in-space degradation with thermal energy plasma exposure for polymers that develop protective oxides, was performed by comparing atomic force microscopy results from silicone samples from EOIM-III (Environmental Oxygen Interaction

with Materials-III) with asher exposed samples. The change in indent force per indent distance was determined for these materials and pristine silicone. Thus, one can then argue that the rate of degradation in space differs from the rate of degradation in thermal energy plasma by the ratio of the atomic oxygen fluences necessary to cause the same indent force per indent distance (or same elastic modulus). This calibration should be valid only for identical or very similar behaving materials. Thus, one would not necessarily expect these same relative rates of degradation to apply for other polymers such as PAEBI's which would have to be separately calibrated by both in-space and ground laboratory testing. For this particular study, DC-93-500 silicone was used for the in-space and RF plasma asher exposure.

Atomic force microscopy measurements were made using a Park Scientific Instruments Auto-Probe atomic force microscope with a micro-indenter having a tip with a radius of curvature of approximately 100 Å. The pristine and EOIM-III space exposed DC-93-500 silicone samples were approximately 0.8 mm thick. The asher exposed DC-93-500 silicone sample was approximately 1 mm thick.

All the thermal energy atomic oxygen exposure ground laboratory testing for data presented in this paper was carried out in Structure Probe, Inc., 100 watt plasma ashers operated on air.

## RESULTS AND DISCUSSION

### Protected Polymers Which Produce Volatile Oxides

The pin window defect in the aluminized Kapton sample retrieved from the LDEF spacecraft, which most closely matched that of the sample which was exposed to atomic oxygen in the plasma asher, had a cross-sectional area of  $0.378 \pm 0.009 (\mu\text{m})^2$ . The defect in the aluminized sample exposed in the plasma asher had an area of  $0.345 \pm 0.012 (\mu\text{m})^2$ . Figure 5 shows scanning electron microscope photographs of the pin-window defects in the aluminized coatings for the LDEF retrieved and asher exposed samples. The LDEF sample was exposed to an atomic oxygen fluence of  $7.15 \times 10^{21}$  atoms/cm<sup>2</sup> with atomic oxygen at 38.1° from normal incidence. The RF plasma asher exposed sample was exposed to the same effective atomic oxygen fluence but with isotropic oxygen arrival.

After the aluminized coating was chemically removed, further scanning electron microscope photographs were taken of both the LDEF retrieved and plasma asher exposed samples as can be seen in Figures 6a and 6b, respectively.

The undercut volume of the LDEF retrieved sample was determined by documentation of the shape of the cavity as a function of depth by means of triangulation based on scanning electron microscope photographs taken at slightly different angles with the assistance of a speck at the bottom of the cavity. The shape of the LDEF retrieved sample was modeled as a truncated oblique cone with a hemisphere at its bottom tip. Resulting computed volume for this undercut area was  $73 \pm 20 (\mu\text{m})^3$ . The asher exposed sample was also modeled using triangulation with the assistance of tiny specks on the crater surface. The depth of the crater as a function of



distance from the axis of the pin window defect was found to match a quadratic equation. The resulting predicted volume for the asher exposed undercut cavity was  $13,000 \pm 2700 (\mu\text{m})^3$ . As one can see, the asher exposed sample had a significantly greater undercut volume than the LDEF sample for the same effective atomic oxygen fluence. A section view comparison of the undercut cavities associated with the LDEF retrieved sample and the RF plasma asher exposed samples is shown in Figure 7. The ratio of in-space mass loss to ground laboratory thermal energy plasma mass loss was then predicted based on the following equation:

$$C = \frac{V_s A_a}{V_a A_s}$$

where:

- C = ratio of in-space to ground laboratory thermal energy plasma mass loss
- $V_s$  = volume of undercut cavity from space exposed sample
- $V_a$  = volume of undercut cavity from RF plasma asher exposed sample
- $A_a$  = area of pin-window defect in aluminized coating on Kapton sample exposed  
in RF plasma asher
- $A_s$  = area of pin-window defect in aluminized coating on sample exposed  
in space on LDEF

If the above equation is the ratio of the undercut cavity volumes corrected for slight differences in pin window defect areas, substituting experimentally observed values for the variables results in:

$$C = \frac{(73 \pm 20) (0.345 \pm 0.012)}{(13000 \pm 2700) (0.378 \pm 0.009)}$$

or  $C = 0.005 \pm 0.002$

Thus, based on volume-derived mass loss comparison of undercut cavities from in-space exposure and in RF plasma ashers the durability of protected polymers in space should be  $1/C$  or  $200 \pm 80$  times that observed in RF plasma ashers. Although this number may be most reliable where protected polymers have defects of approximately the same area as examined here, the estimates of the average defect diameter for  $\text{SiO}_x$  protected Kapton indicate average defect diameters of  $1.56 \mu\text{m}$  (Ref. 15). This average defect diameter is not unreasonably different from the measured LDEF defect which would have a diameter equivalent to  $0.69 \mu\text{m}$  based on a circular defect equivalent in area to the measured LDEF defect. The above predicted in-space relative mass loss or relative durability between in-space and ground laboratory thermal energy plasma exposure results are in reasonable agreement with the value of .0056 as measured with  $\text{SiO}_2$  protective films on Kapton H during a low fluence shuttle in-

bay exposure (Ref. 11), and high effective fluence ( $8.99 \times 10^{21}$  atoms/cm<sup>2</sup>) plasma asher exposure of similar SiOx coated Kapton H (Ref. 16).

### Polymers That Develop Protective Oxides

The results of atomic force microscopy micro-indenter measurements of DC-93-500 silicone exposed to various fluences of atomic oxygen is shown in Figure 8. The graph compares the ground laboratory RF plasma asher exposed, and in-space EOIM-III exposed pristine DC-93-500 silicone to bulk fused silica. At zero fluence the plasma asher and EOIM-III silicone has low elastic modulus characteristics as indicated by the small indent force per indent distance. As the atomic oxygen fluence increases a greater fraction of the surface of the silicone is converted to silica and to a greater depth. This causes the silicones to become more rigid on their surface as previously mentioned. Although it is believed that the indent force per indent distance would continue to increase with fluence in excess of that shown on the plot. The indent force per indent distance should not reach the value for bulk fused silica because the resulting silica on the converted silicone surface should be more porous than that of bulk fused silica. This is due to the oxidation process involving the loss of volatile methyl groups as a result of atomic oxygen attack. The loss of these hydrocarbon groups would tend to make the oxidized silicone surface microscopically porous and as such would be more compliant than bulk fused silica.

The atomic oxygen fluence measured in the asher was based on Kapton H effective fluence. The ratio of in-space durability to RF plasma asher durability is given simply by the ratio of plasma asher effective fluence to in-space asher fluence which is necessary to produce the same indent force per indent distance. The curve fit for the plasma asher data with an effective fluence of  $0.23 \times 10^{20}$  atoms/cm<sup>2</sup> produces the same surface as occurred on EOIM-III which was exposed to an atomic oxygen fluence of  $2.3 \times 10^{20}$  atoms/cm<sup>2</sup>. Thus, the ratio of in-space to thermal energy plasma asher durability for DC-93-500 silicone is given by

$$C = \frac{0.235 \times 10^{20} \text{ atoms/cm}^2}{2.3 \times 10^{20} \text{ atoms/cm}^2}$$

or  $C = 0.1$

The uncertainty in the above in-space to thermal energy plasma degradation ratio is purposely not listed because the uncertainty of the indent force per indent distance data is currently not known. Based on the results to date of the indent force per indent distance data, it appears that the accuracy of this technique can be improved with proper selection of the indenter stylus, as well as the applied indenter force. The above analysis allows one to compare the relative rates of degradation, however the absolute durability depends on what criteria one places on the performance of the particular material that develops a protective oxide. For example, the criteria may be tensile failure of the material, micro-cracking of the surface due to oxidation or a specified loss in specular transmittance of the material. Samples of DC-93-500 silicone develop surface micro-cracking with atomic oxygen exposure. The EOIM-III sample had surface

micro-cracking at a fluence of  $2.3 \times 10^{20}$  atoms/cm<sup>2</sup> (Ref. 6) and the RF plasma asher exposed samples have shown evidence of surface micro-cracking at fluences as low as  $6.5 \times 10^9$  atoms/cm<sup>2</sup>. If the relative rates between thermal energy plasma and in-space degradation occur consistent with the comparison of indent force per indent distance measurements, then one simply would have to expose samples in the RF plasma asher to a fluence that causes the material to perform unacceptably and then apply this in-space to thermal energy plasma ratio to determine how much fluence in space would be necessary to cause the material to degrade to the same condition. As previously mentioned, it is also believed that the results for this particular silicone will be unique to that particular material and that other materials such as PAEBI's will require their own in-space and RF plasma asher characterization to determine their relative in-space to thermal energy plasma degradation rates.

## SUMMARY

Quantified estimates of the ratio of in-space atomic oxygen durability to ground laboratory thermal energy plasma durability was made by comparing results of LDEF and EOIM-III in-space exposure of identical materials in RF plasma ashers. The study conducted for two types of materials: protected polymers that produce volatile oxides and polymers that develop protective oxides. To investigate protected polymers, a sample of aluminized Kapton H retrieved from LDEF was compared with RF plasma asher results of atomic oxygen undercutting at nearly identical area defect sites in the aluminized protective coating. By comparison of the undercut cavities it was found that the degradation in space (mass loss) was  $0.005 \pm 0.002$  that which occurs in an RF plasma asher for samples exposed to the same effective atomic oxygen fluence.

A similar comparison of relative rates of degradation in space compared to RF plasma asher degradation was made for polymers that develop protective oxides. The particular material selected for this investigation was DC-93-500 silicone. Atomic force microscopy indent techniques were used to characterize the degree of conversion of the surface from silicone to silica by measuring the stylus indent force per indent pressure as a function of fluence. By comparison of the same indent force per indent distance characteristics, it was determined that the rate of in-space degradation of DC-93-500 silicone, is approximately 1/10 of that which occurs in RF plasma ashers for the same effective fluence.

## REFERENCES

1. Rutledge, S. K., Olle, R. and Cooper, J., "Atomic Oxygen Effects on SiO<sub>x</sub> coated Kapton for photovoltaic arrays in low Earth orbit," paper presented at the IEEE Photovoltaic Specialists Conference, Las Vegas, NV, October 7-11, 1991.
2. Banks, B. A., Rutledge, S. K., de Groh, K. K., "Low Earth Orbital Atomic Oxygen, Micrometeoroid, and Debris Interactions with Photovoltaic Arrays," paper presented at the 11th Space Photovoltaic Research and Technology Conference (SPRAT XI), NASA Lewis Research Center, Cleveland, OH, May 7-9, 1991.

3. de Groh, K. K., and Banks, B. A., "Atomic Oxygen Undercutting of Long Duration Exposure Facility Aluminized-Kapton Multilayer Insulation," *J. Spacecraft and Rockets*, Vol. 31, No. 4, p. 656-664, August, 1994.
4. Banks, B.A., Dever, J.A., Gebauer, L. and Hill, C.M., "Atomic Oxygen Interactions with FEP Teflon and Silicones on LDEF," *Proceedings of the First LDEF Post-Retrieval Symposium*, Kissimmee, FL, June 2-8, 1991, pp. 801-815.
5. Hung, C., and Cantrell, G., "Reaction and Protection of Electrical Wire Insulators in Atomic Oxygen Environment", NASA TM 106767, April 12-14, 1994.
6. de Groh, K.K. and McCollum, T.A., "Low Earth Orbit Durability of Protected Silicone for Refractive Photovoltaic Concentrator Arrays", *J. Spacecraft and Rockets*, vol. 32, No. 1, pp. 103-109, January-February, 1995.
7. Banks, B. A., Auer, B., and DiFilippo, F. J., "Atomic Oxygen Undercutting of Defects on SiO<sub>2</sub> Protected Polyimide Solar Array Blankets", in Materials Degradation in Low Earth Orbit (LEO), Srinivasan, V. And Banks, B. A., eds., *Proceedings of Symposium sponsored by the TMS, ASM Joint Corrosion and Environmental Effects Committee, held at the 119th Annual Meeting of the Minerals, Metals and Materials Society, in Anaheim, CA, February 17-22, 1990.*
8. Ferguson, D.C., "The Energy Dependence of Surface Morphology of Kapton Degradation Under Atomic Oxygen Bombardment", paper presented at the 13th Space Simulation Conference, Orlando, FL, October 8-11, 1984.
9. Krech, R., "Determination of Oxygen Erosion Yield Dependencies upon Specific LEO Environments", NASA Contractor Report No. NAS3-25968, March, 1993.
10. Banks, B.A., Rutledge, S.K., de Groh, K.K., Stidham, C. R., Gebauer, L., and LaMoureaux, C., "Atomic Oxygen Durability Evaluation of Protected Polymers using Thermal Energy Plasma Systems", NASA TM 106855, presented at the International Conference on Plasma Synthesis and Processing of Materials, sponsored by the Metallurgical Society, Denver, CO, February 21-15, 1993.
11. Banks, B.A., Mirtich, M. J., Rutledge, S.K., and Swec, D.I, "Sputtered Coatings for Protection of Spacecraft Polymers", NASA TM 83706, presented at the 11th International Conference on Metallurgical Coatings, sponsored by the American Vacuum Society, San Diego, CA, April 9-13, 1984.
12. Whitaker, A., NASA Marshall Space Flight Center personal communication.

13. Banks, B.A., and Gebauer, L., "LDEF Yaw and Pitch Angle Estimates", proceedings of the LDEF Materials Results for Spacecraft Applications conference, Huntsville, AL, Oct. 27-28, 1992.
14. Stein, B., "LDEF Materials Overview", LDEF-69 Months in Space, Second Post-Retrieval Symposium, NASA CP-3194, Part III, June 1992.
15. Banks, B. A., Rutledge, S. K., and Gebauer, L., "SiO<sub>x</sub> Coatings for Atomic Oxygen Protection of Polyimide Kapton in Low Earth Orbit", AIAA paper 92-2151, presented at the Coating Technologies for Aerospace Systems Materials Specialist Conference, Dallas, TX, April 16-17, 1992.
16. Rutledge, S. K. and Mihelcic, J. A., "The Effect of Atomic Oxygen on Altered and Coated Kapton Surfaces for Spacecraft Applications in Low Earth Orbit", in Materials Degradation in Low Earth Orbit (LEO), Srinivasan, V. and Banks, B.A., eds., Symposium sponsored by the TMS-ASM Joint Corrosion and Environmental Effects Committee held at the 119th Annual Meeting of the Minerals, Metals and Materials Society in Anaheim, CA, Feb. 17-22, 1990.

Table 1. Atomic oxygen flux relative to that at normal incidence for a 400 km orbit inclined at 28.5° and a 996 K atmosphere.

Angle from normal incidence, degrees	Flux relative to normal flux measured in a plane	
	Parallel to the Earth's Horizon	Perpendicular to the Earth's Horizon
0	1.00	1.00
1	$9.88 \times 10^{-1}$	$9.87 \times 10^{-1}$
2	$9.52 \times 10^{-1}$	$9.50 \times 10^{-1}$
3	$8.95 \times 10^{-1}$	$8.90 \times 10^{-1}$
4	$8.21 \times 10^{-1}$	$8.13 \times 10^{-1}$
5	$7.34 \times 10^{-1}$	$7.24 \times 10^{-1}$
6	$6.41 \times 10^{-1}$	$6.29 \times 10^{-1}$
7	$5.45 \times 10^{-1}$	$5.32 \times 10^{-1}$
8	$4.55 \times 10^{-1}$	$4.39 \times 10^{-1}$
9	$3.69 \times 10^{-1}$	$3.54 \times 10^{-1}$
10	$2.93 \times 10^{-1}$	$2.78 \times 10^{-1}$
11	$2.27 \times 10^{-1}$	$2.13 \times 10^{-1}$
12	$1.72 \times 10^{-1}$	$1.59 \times 10^{-1}$
13	$1.27 \times 10^{-1}$	$1.16 \times 10^{-1}$
14	$9.17 \times 10^{-2}$	$8.31 \times 10^{-2}$
15	$6.48 \times 10^{-2}$	$5.80 \times 10^{-2}$
16	$4.48 \times 10^{-2}$	$3.95 \times 10^{-2}$
17	$3.03 \times 10^{-2}$	$2.64 \times 10^{-2}$
18	$2.00 \times 10^{-2}$	$1.72 \times 10^{-2}$
19	$1.30 \times 10^{-2}$	$1.10 \times 10^{-2}$
20	$8.25 \times 10^{-3}$	$6.89 \times 10^{-3}$
21	$5.14 \times 10^{-3}$	$4.23 \times 10^{-3}$

	Flux relative to normal flux measured in a plane	
Angle from normal incidence, degrees	Parallel to the Earth's Horizon	Perpendicular to the Earth's Horizon
22	$3.14 \times 10^{-3}$	$2.54 \times 10^{-3}$
23	$1.89 \times 10^{-3}$	$1.50 \times 10^{-3}$
24	$1.10 \times 10^{-3}$	$8.70 \times 10^{-4}$
25	$6.38 \times 10^{-4}$	$4.95 \times 10^{-4}$
26	$3.62 \times 10^{-4}$	$2.77 \times 10^{-4}$
27	$2.02 \times 10^{-4}$	$1.53 \times 10^{-4}$
28	$1.11 \times 10^{-4}$	$8.27 \times 10^{-5}$
29	$5.60 \times 10^{-5}$	$4.42 \times 10^{-5}$
30	$3.20 \times 10^{-5}$	$2.32 \times 10^{-5}$
31	$1.68 \times 10^{-5}$	$1.21 \times 10^{-5}$
32	$8.70 \times 10^{-6}$	$6.18 \times 10^{-6}$
33	$4.45 \times 10^{-6}$	$3.13 \times 10^{-6}$
34	$2.25 \times 10^{-6}$	$1.57 \times 10^{-6}$
35	$1.12 \times 10^{-6}$	$7.76 \times 10^{-7}$
36	$5.56 \times 10^{-7}$	$3.80 \times 10^{-7}$
37	$2.72 \times 10^{-7}$	$1.85 \times 10^{-7}$
38	$1.32 \times 10^{-7}$	$8.91 \times 10^{-8}$
39	$6.36 \times 10^{-8}$	$4.26 \times 10^{-8}$
40	$3.04 \times 10^{-8}$	$2.03 \times 10^{-8}$
41	$1.44 \times 10^{-8}$	$9.57 \times 10^{-9}$
42	$6.81 \times 10^{-9}$	$4.50 \times 10^{-9}$
43	$3.20 \times 10^{-9}$	$2.11 \times 10^{-9}$
44	$1.50 \times 10^{-9}$	$9.84 \times 10^{-10}$
45	$6.97 \times 10^{-10}$	$4.58 \times 10^{-10}$

	Flux relative to normal flux measured in a plane	
Angle from normal incidence, degrees	Parallel to the Earth's Horizon	Perpendicular to the Earth's Horizon
46	$3.24 \times 10^{-10}$	$2.13 \times 10^{-10}$
47	$1.50 \times 10^{-10}$	$9.88 \times 10^{-11}$
48	$6.97 \times 10^{-11}$	$4.59 \times 10^{-11}$
49	$3.23 \times 10^{-11}$	$2.13 \times 10^{-11}$
50	$1.50 \times 10^{-11}$	$9.93 \times 10^{-12}$
51	$6.95 \times 10^{-12}$	$4.63 \times 10^{-12}$
52	$3.24 \times 10^{-12}$	$2.17 \times 10^{-12}$
53	$1.51 \times 10^{-12}$	$1.02 \times 10^{-12}$
54	$7.09 \times 10^{-13}$	$4.81 \times 10^{-13}$
55	$3.34 \times 10^{-13}$	$2.28 \times 10^{-13}$
56	$1.58 \times 10^{-13}$	$1.09 \times 10^{-13}$
57	$7.54 \times 10^{-14}$	$5.24 \times 10^{-14}$
58	$3.62 \times 10^{-14}$	$2.54 \times 10^{-14}$
59	$1.75 \times 10^{-14}$	$1.24 \times 10^{-14}$
60	$8.53 \times 10^{-15}$	$6.12 \times 10^{-15}$
61	$4.20 \times 10^{-15}$	$2.94 \times 10^{-15}$
62	$2.09 \times 10^{-15}$	$1.53 \times 10^{-15}$
63	$1.05 \times 10^{-15}$	$7.78 \times 10^{-16}$
64	$5.32 \times 10^{-16}$	$4.00 \times 10^{-16}$
65	$2.73 \times 10^{-16}$	$2.08 \times 10^{-16}$
66	$1.41 \times 10^{-16}$	$1.10 \times 10^{-16}$
67	$7.47 \times 10^{-17}$	$5.84 \times 10^{-17}$
68	$3.98 \times 10^{-17}$	$3.15 \times 10^{-17}$
69	$2.15 \times 10^{-17}$	$1.73 \times 10^{-17}$



Angle from normal incidence, degrees	Flux relative to normal flux measured in a plane	
	Parallel to the Earth's Horizon	Perpendicular to the Earth's Horizon
70	$1.18 \times 10^{-17}$	$9.90 \times 10^{-18}$
71	$6.57 \times 10^{-18}$	$5.41 \times 10^{-18}$
72	$3.71 \times 10^{-18}$	$3.09 \times 10^{-18}$
73	$2.13 \times 10^{-18}$	$1.79 \times 10^{-18}$
74	$1.24 \times 10^{-18}$	$1.06 \times 10^{-18}$
75	$7.35 \times 10^{-19}$	$6.31 \times 10^{-19}$
76	$4.43 \times 10^{-19}$	$3.83 \times 10^{-19}$
77	$2.72 \times 10^{-19}$	$2.36 \times 10^{-19}$
78	$1.70 \times 10^{-19}$	$1.48 \times 10^{-19}$
79	$1.08 \times 10^{-19}$	$9.37 \times 10^{-20}$
80	$7.00 \times 10^{-20}$	$6.04 \times 10^{-20}$
81	$4.63 \times 10^{-20}$	$3.98 \times 10^{-20}$
82	$3.12 \times 10^{-20}$	$2.62 \times 10^{-20}$
83	$2.15 \times 10^{-20}$	$1.77 \times 10^{-20}$
84	$1.50 \times 10^{-20}$	$1.21 \times 10^{-20}$
85	$1.07 \times 10^{-20}$	$8.36 \times 10^{-21}$
86	$7.69 \times 10^{-21}$	$5.87 \times 10^{-21}$
87	$5.56 \times 10^{-21}$	$4.18 \times 10^{-21}$
88	$3.98 \times 10^{-21}$	$3.01 \times 10^{-21}$
89	$2.73 \times 10^{-21}$	$2.20 \times 10^{-21}$
90	$1.66 \times 10^{-21}$	$1.62 \times 10^{-21}$

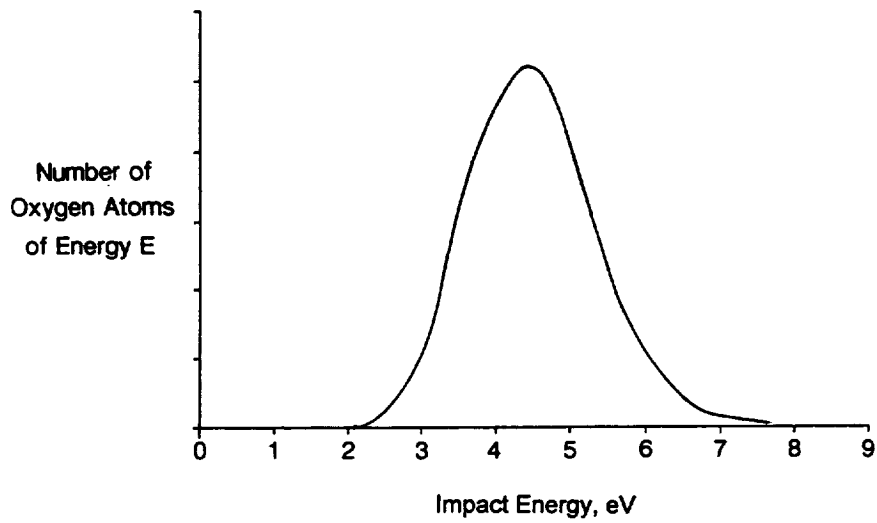


Figure 1. Low Earth orbital atomic oxygen energy distribution.

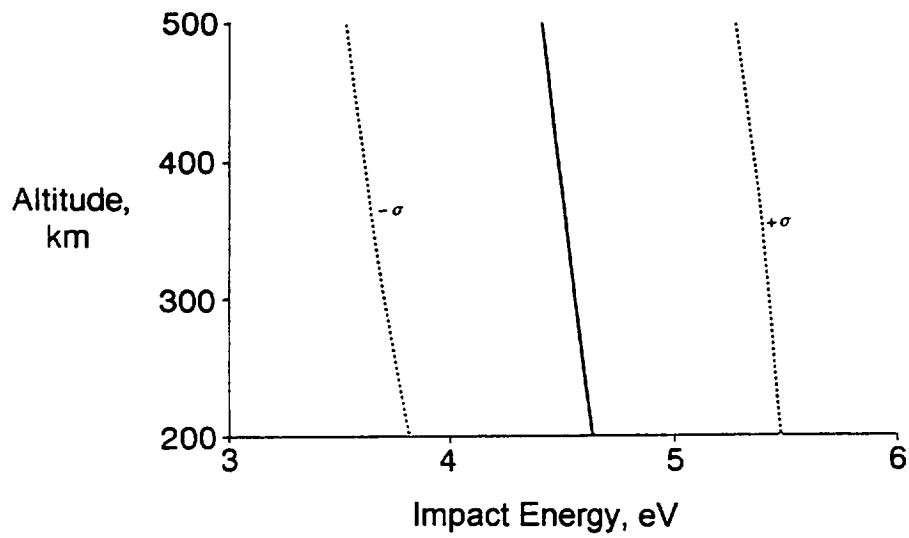


Figure 2. Low Earth orbital atomic oxygen mean and +/- sigma energy as a function of altitude for a 28.5° inclined orbit, assuming 996 K atmosphere.

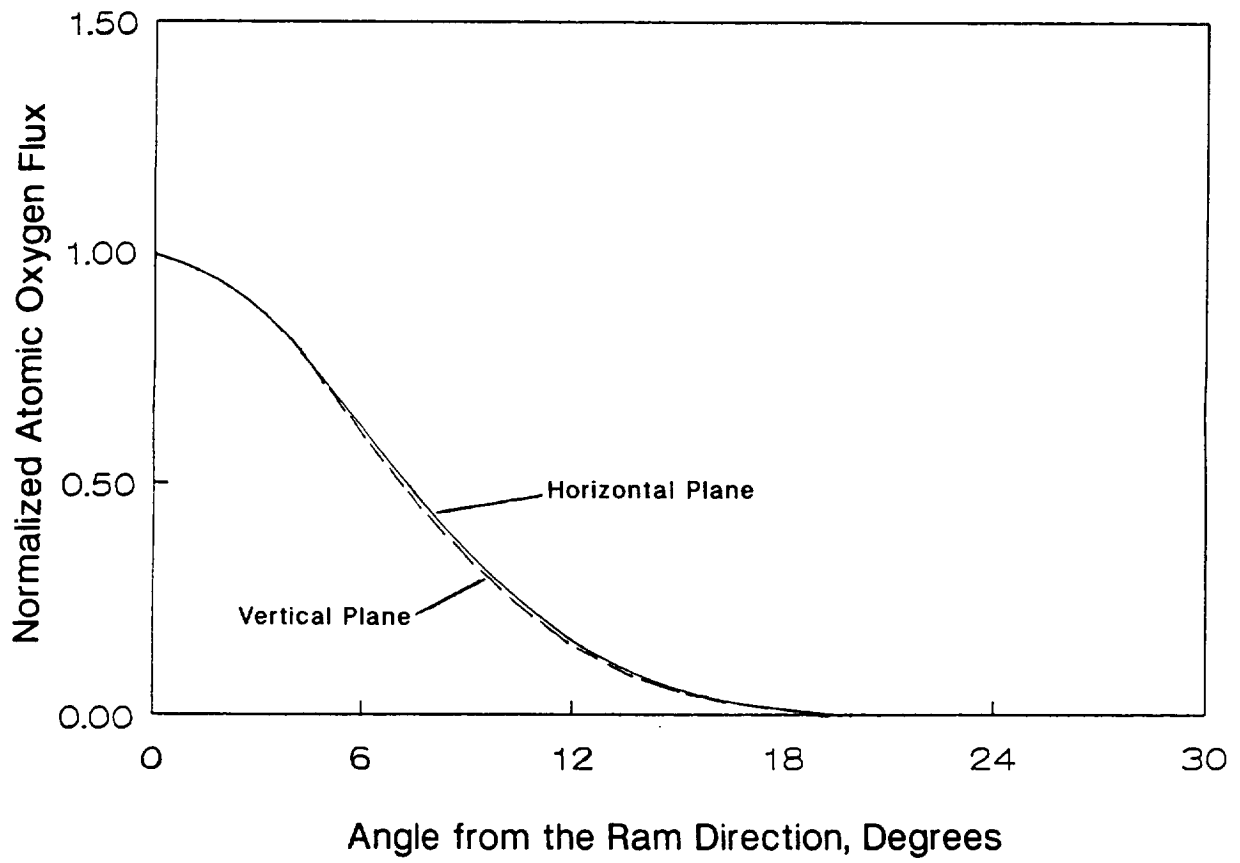


Figure 3. Angular distribution of arriving atomic oxygen flux for both in a plane parallel to the Earth's horizon as well as a plane perpendicular to the Earth's horizon

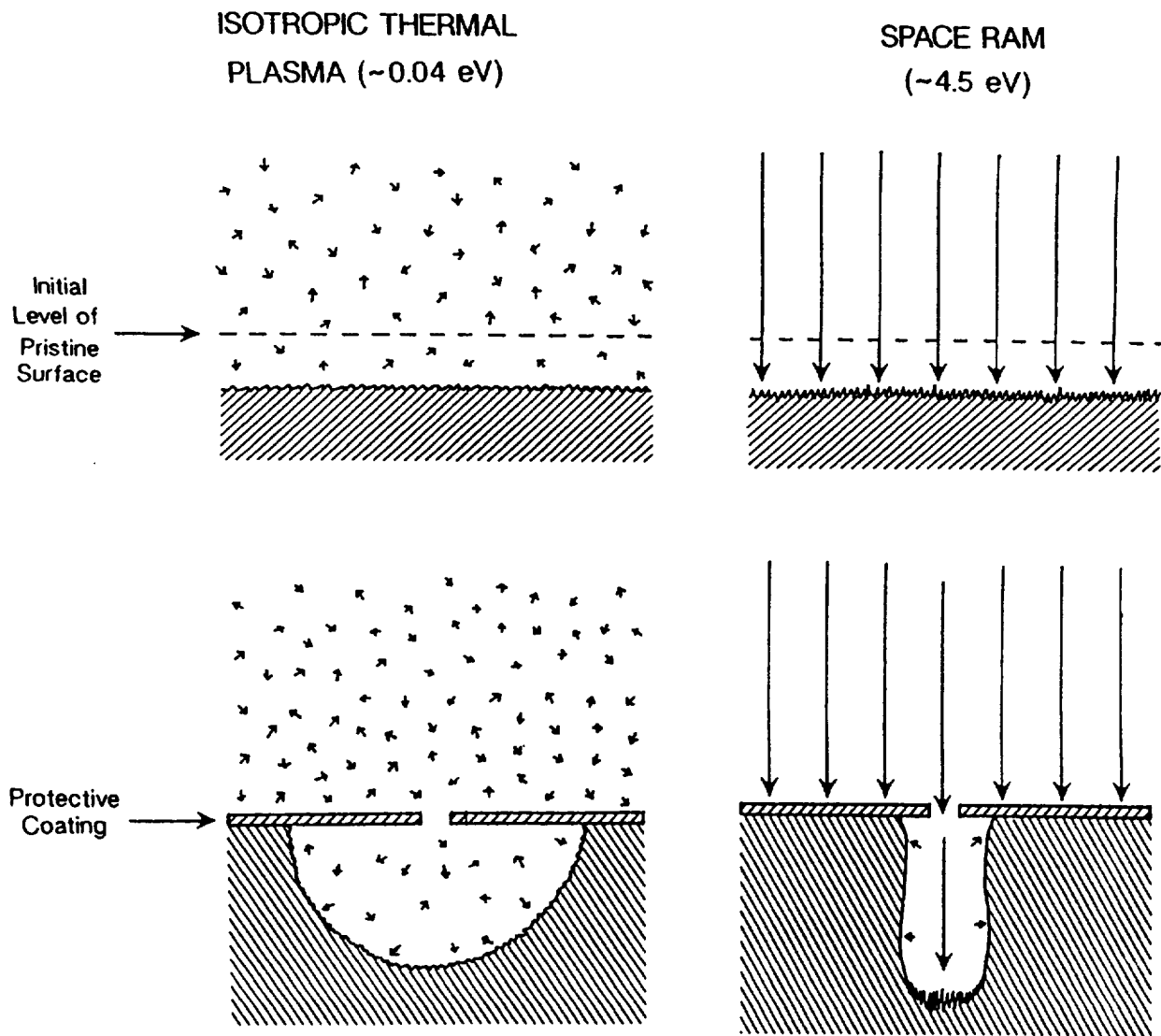
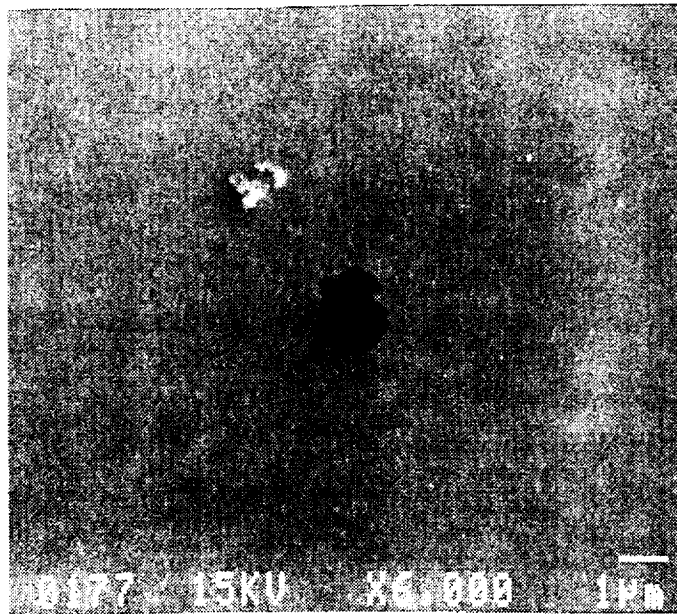


Figure 4. Illustration of the differences in atomic oxygen undercutting of protected polymers between the LEO environment and an isotropic thermal energy plasma environment for the same amount of unprotected material loss (same equivalent fluence).

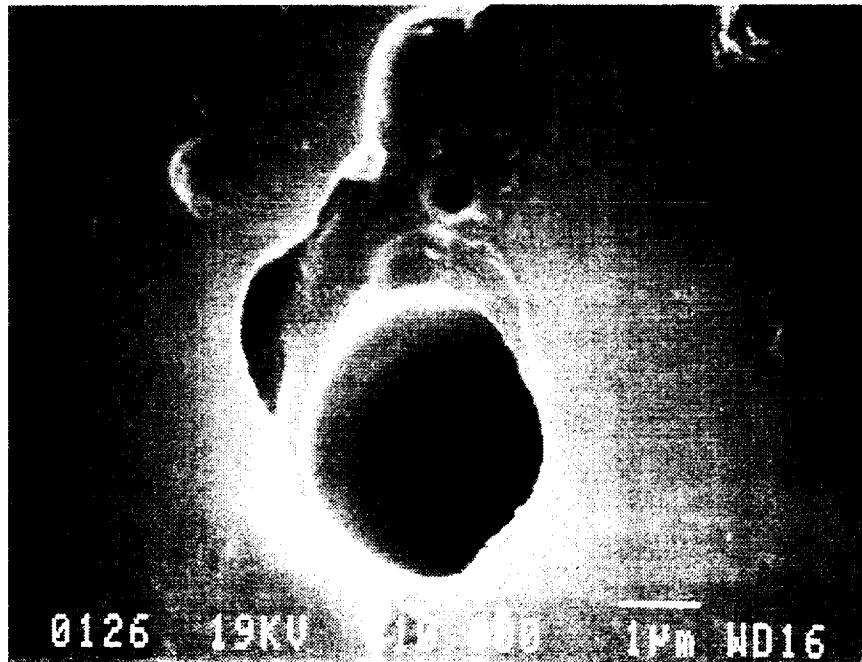


5a. LDEF retrieved sample

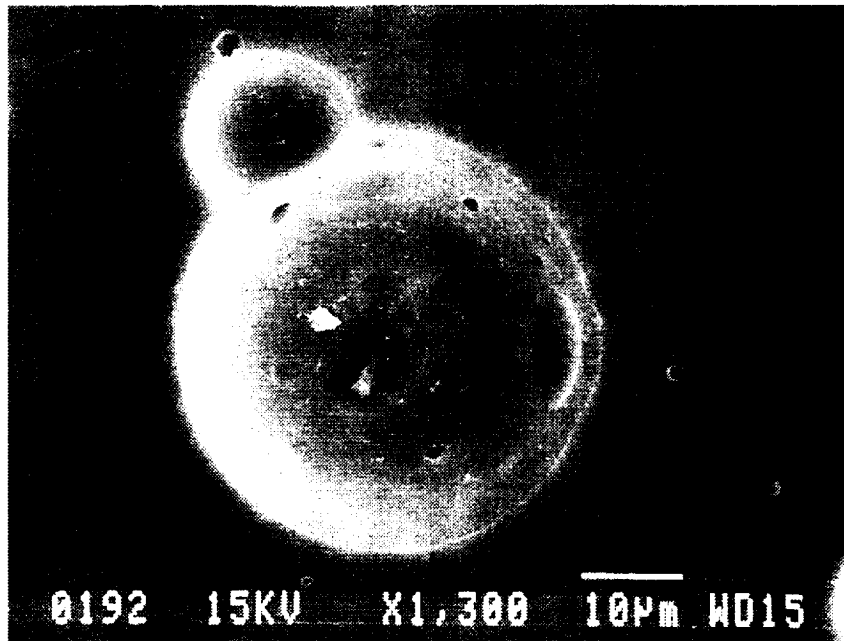


5b. RF plasma asher exposed sample

Figure 5. Pin-window defects in aluminized Kapton after atomic oxygen exposure.



6a. LDEF retrieved sample



6b. RF plasma asher exposed sample

Figure 6. Scanning electron microscope photographs of undercut cavities taken after chemical removal of the aluminized film at the defect sites shown respectively in Figures 5a and 5b.

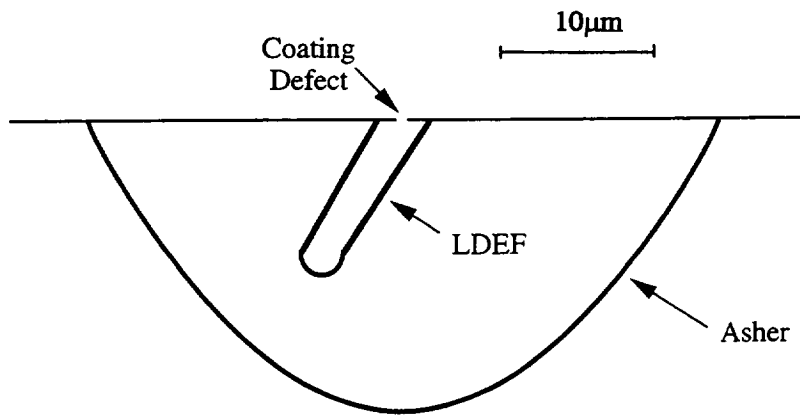


Figure 7. A comparison of an undercut cavity associated with similar defects in aluminized Kapton exposed on LDEF and in an RF plasma asher to a fluence of  $7.15 \times 10^{21}$  atoms/cm<sup>2</sup>.

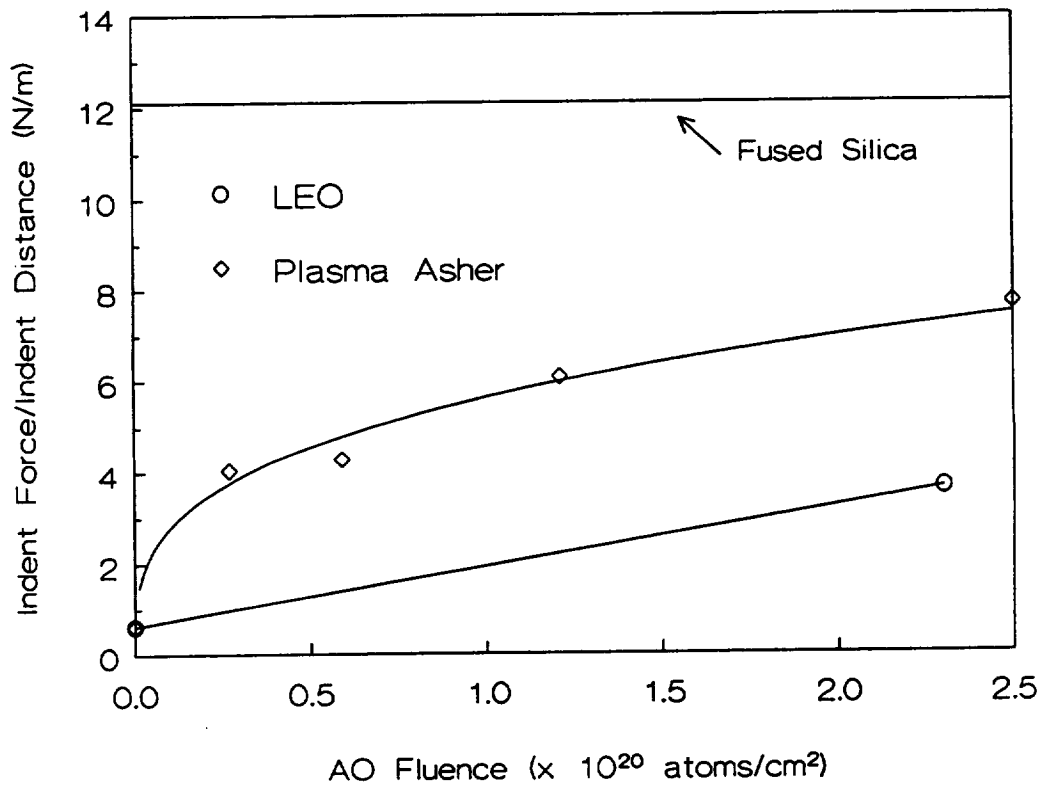


Figure 8. Atomic force microscopy indent force per indent distance as a function of atomic oxygen fluence for RF plasma asher and EOIM-III in-space exposed DC-93-500 silicone samples.

**REPORT DOCUMENTATION PAGE**Form Approved  
OMB No. 0704-0188

Public reporting burden for this collection of information is estimated to average 1 hour per response, including the time for reviewing instructions, searching existing data sources, gathering and maintaining the data needed, and completing and reviewing the collection of information. Send comments regarding this burden estimate or any other aspect of this collection of information, including suggestions for reducing this burden, to Washington Headquarters Services, Directorate for Information Operations and Reports, 1215 Jefferson Davis Highway, Suite 1204, Arlington, VA 22202-4302, and to the Office of Management and Budget, Paperwork Reduction Project (0704-0188), Washington, DC 20503.

<b>1. AGENCY USE ONLY (Leave blank)</b>		<b>2. REPORT DATE</b> April 1996	<b>3. REPORT TYPE AND DATES COVERED</b> Technical Memorandum	
<b>4. TITLE AND SUBTITLE</b> Prediction of In-Space Durability of Protected Polymers Based on Ground Laboratory Thermal Energy Atomic Oxygen			<b>5. FUNDING NUMBERS</b>  WU-233-1A-1E	
<b>6. AUTHOR(S)</b> Bruce A. Banks, Kim K. de Groh, Sharon K. Rutledge, and Frank J. DiFilippo				
<b>7. PERFORMING ORGANIZATION NAME(S) AND ADDRESS(ES)</b> National Aeronautics and Space Administration Lewis Research Center Cleveland, Ohio 44135-3191			<b>8. PERFORMING ORGANIZATION REPORT NUMBER</b>  E-10225	
<b>9. SPONSORING/MONITORING AGENCY NAME(S) AND ADDRESS(ES)</b> National Aeronautics and Space Administration Washington, D.C. 20546-0001			<b>10. SPONSORING/MONITORING AGENCY REPORT NUMBER</b>  NASA TM-107209	
<b>11. SUPPLEMENTARY NOTES</b> Prepared for the Third International Conference for the Protection of Materials and Structures from the LEO Space Environment, Toronto, Canada, April 25-26, 1996. Bruce A. Banks, Kim K. de Groh, and Sharon K. Rutledge, NASA Lewis Research Center; Frank J. DiFilippo, Case Western Reserve University, Cleveland, Ohio. Responsible person, Bruce A. Banks, organization code 5480, (216) 433-2308.				
<b>12a. DISTRIBUTION/AVAILABILITY STATEMENT</b>  Unclassified - Unlimited Subject Category 27  This publication is available from the NASA Center for Aerospace Information, (301) 621-0390.			<b>12b. DISTRIBUTION CODE</b>	
<b>13. ABSTRACT (Maximum 200 words)</b>  The probability of atomic oxygen reacting with polymeric materials is orders of magnitude lower at thermal energies (<0.1 eV) than at orbital impact energies (4.5 eV). As a result, absolute atomic oxygen fluxes at thermal energies must be orders of magnitude higher than orbital energy fluxes, to produce the same effective fluxes (or same oxidation rates) for polymers. These differences can cause highly pessimistic durability predictions for protected polymers and polymers which develop protective metal oxide surfaces as a result of oxidation if one does not make suitable calibrations. A comparison was conducted of undercut cavities below defect sites in protected polyimide Kapton samples flown on the Long Duration Exposure Facility (LDEF) with similar samples exposed in thermal energy oxygen plasma. The results of this comparison were used to quantify predicted material loss in space based on material loss in ground laboratory thermal energy plasma testing. A microindent hardness comparison of surface oxidation of a silicone flown on the Environmental Oxygen Interaction with Materials-III (EOIM-III) experiment with samples exposed in thermal energy plasmas was similarly used to calibrate the rate of oxidation of silicone in space relative to samples in thermal energy plasmas exposed to polyimide Kapton effective fluences.				
<b>14. SUBJECT TERMS</b> Oxygen atoms; Protective coatings; Thermal energy; Kapton; Silicone; Aerospace environments			<b>15. NUMBER OF PAGES</b> 24	
			<b>16. PRICE CODE</b> A03	
<b>17. SECURITY CLASSIFICATION OF REPORT</b> Unclassified	<b>18. SECURITY CLASSIFICATION OF THIS PAGE</b> Unclassified	<b>19. SECURITY CLASSIFICATION OF ABSTRACT</b> Unclassified	<b>20. LIMITATION OF ABSTRACT</b>	





**National Aeronautics and  
Space Administration**

**Lewis Research Center**  
21000 Brookpark Rd.  
Cleveland, OH 44135-3191

Official Business  
Penalty for Private Use \$300

POSTMASTER: If Undeliverable — Do Not Return